ℓ_2 OPTIMIZED PREDICTIVE IMAGE CODING WITH ℓ_∞ BOUND

Sceuchin Chuah, Sorina Dumitrescu and Xiaolin Wu

Department of Electrical and Computer Engineering
McMaster University, Hamilton, Canada
E-mails: chuahs@mcmaster.ca, sorina@mail.ece.mcmaster.ca and xwu@mail.ece.mcmaster.ca

ABSTRACT

In many scientific, medical and defense applications of image/video compression, an ℓ_∞ error bound is required. However, pure ℓ_∞-optimized image coding, colloquially known as near-lossless image coding, is prone to structured errors such as contours and speckles if the bit rate is not sufficiently high; moreover, previous ℓ_∞-based image coding methods suffer from poor rate control. In contrast, the ℓ_2 error metric aims for average fidelity and hence preserves the subtlety of smooth waveforms better than the ℓ_∞ error metric and it offers fine granularity in rate control; but pure ℓ_2-based image coding methods (e.g., JPEG 2000) cannot bound individual errors as the ℓ_∞-based methods can. This paper presents a new compression approach to retain the benefits and circumvent the pitfalls of the two error metrics.

1. INTRODUCTION

For many important applications of image compression in science, medicine, space exploration, precision engineering, etc., high fidelity of image reconstruction is required. The ideal solution is lossless compression, but this demands a relatively high bit budget. A practical alternative is ℓ_∞-constrained image coding.

A straightforward method of ℓ_∞-constrained image compression is a cascade of uniform scalar quantization of all pixel values followed by lossless coding of the pre-quantized image [1, 2]. But a far more efficient near-lossless coding approach is a closed loop of a causal DPCM predictor and uniform scalar quantizer of prediction residuals [3, 4, 5]. Both the techniques of [3] and [4] are based on the DPCM method. In [3] a uniform (or a nearly uniform) scalar quantizer is used to quantize the prediction errors, while in [4], a mechanism to minimize the entropy of the sequence of quantized prediction residues is incorporated. Finally, ℓ_∞-constrained (or near-lossless) CALIC [5] is a variant of lossless CALIC [6] and it uses a uniform scalar quantizer for the residual errors in the prediction loop. Among the aforementioned ℓ_∞-constrained image coders, near-lossless CALIC achieves the highest compression performance when $\tau \leq 3$ [5]. Further enhancements of near-lossless CALIC were proposed in [7, 8], which led to superior performance in terms of bit rate and/or ℓ_2 distortion, but at the expense of increased computational complexity.

The design goal of existing ℓ_∞-constrained image coders is to achieve the lowest bit rate for each given error bound τ, neglecting other operational issues. One side effect is that the number of achievable bit rates is small, only equal to the number of possible values of τ. Such a coarse rate granularity makes it very difficult to finely adjust the bit rate versus the distortion bound. For test image in Fig. 4 as an example, the bit rates achievable by near-lossless CALIC for $\tau = 0, 1, \cdots, 8$, are $3.53, 2.13, 1.57,\ 1.27, 1.07, 0.94, 0.82, 0.73$, 0.67, respectively. Notice the big gaps between consecutive bit rates. In order to improve the reconstruction quality at $\tau = 2$, the only option is to choose $\tau = 1$, but this incurs a big rate increment of 0.56 bpp (or 35.67%). The resulting next higher rate will be wasteful if the reconstruction quality at $\tau = 2$ is just slightly lower than required.

Moreover, the suitability of pure ℓ_∞ distortion metric in preserving image quality may also be put into question. In particular, ℓ_∞-constrained image coders may introduce structured artifacts in smooth regions. Fig. 1 compares images coded by an ℓ_∞-based compression method (near-lossless CALIC with $\tau = 4$) and an ℓ_2-based compression method (JPEG 2000) when the bit rates are the same. As shown in Fig. 1c, the ℓ_∞-constrained CALIC produces contours in smooth shade region. Although the ℓ_2-based JPEG 2000 does not produce contour artifacts, it removes the small feature on the smooth surface as identified in Fig. 1b. In fact, the tendency of ℓ_2-based image coders to distort or even remove small features, which are statistical outliers, motivated the research on ℓ_∞-based image coders. In some important applications, tiny objects (e.g., lesions in medical images or small boats in satellite images) carry great semantic significance even though they are tiny minority statistically speaking.

To summarize the above observations, the ℓ_2 distortion metric, being an average fidelity measure, preserves the subtle smooth image waveforms better; on the other hand, the ℓ_∞ distortion metric, aiming for best minmax approximation, preserves isolated small image features better. The other major difference between the ℓ_2 and ℓ_∞ code design crite-

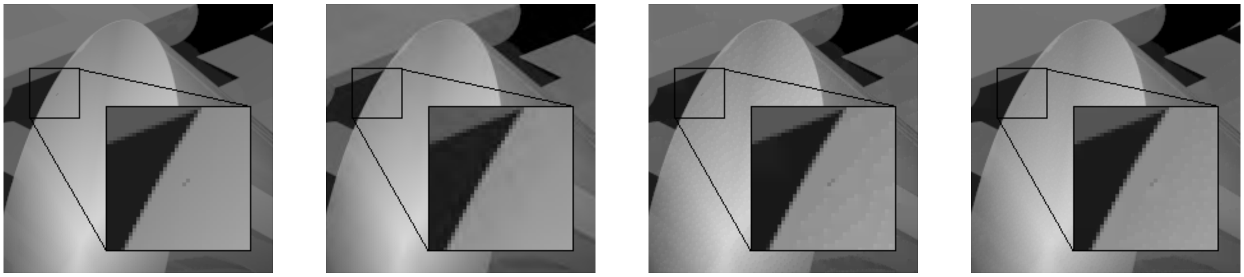

(a) Original image (b) JPEG 2000 (c) Near-lossless CALIC (d) Proposed

Fig. 1. Comparison using a computer-generated test image between (a) Original image / Lossless image coding (Lossless CALIC at rate 1.27 bpp); (b) ℓ_2-based image coding (JPEG 2000 at rate 0.38 bpp, PSNR 42.08dB, ℓ_∞ error bound 22) with the small feature in the smooth region blurred out; (c) ℓ_∞-based image coding (Near-lossless CALIC at rate 0.38 bpp, PSNR 39.45dB, ℓ_∞ error bound 4) with speckles and contours as artifacts; and (d) Proposed method (at rate 0.47 bpp, PSNR 39.63dB, ℓ_∞ error bound 4) preserving the small feature with minimal artifacts.

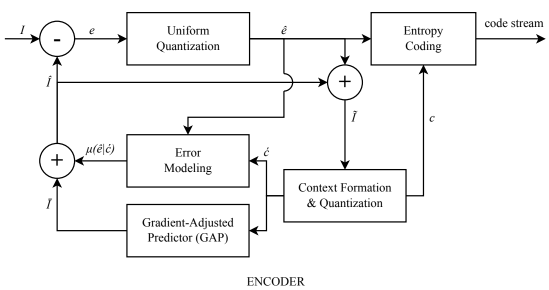

Fig. 2. Flow diagram of near-lossless CALIC.

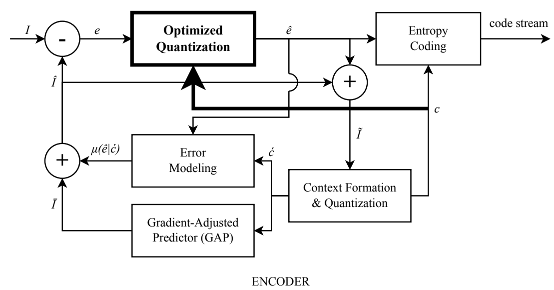

Fig. 3. Flow diagram of the proposed method.

ria is that the former offers much finer rate granularity than the latter. Now a natural inquiry, which is the main theme of this paper, is in order: can one get the advantages of the two metrics but not their shortcomings? Towards this objective, we develop a new technique of incorporating a mechanism of ℓ_2 optimization in the existing framework of ℓ_∞-constrained image coding. Specifically, we modify the near-lossless CALIC system by replacing the previous in-loop uniform scalar quantizer with a set of context-based ℓ_2-optimized scalar quantizers. The main innovations of this work are the formulation of an algorithm for the optimal code design problem of minimizing a weighted sum of the ℓ_2 distortion and the total rate over all possible quantizers, while obeying a specified ℓ_∞ error bound.

What distinguishes our work from previous works on optimal quantizer design is mainly the criterion used in the optimization. Most quantizer design algorithms minimize the ℓ_2 distortion for fixed-rate quantizers [9, 10, 11, 12, 13, 14], or the weighted sum of ℓ_2 distortion and entropy [16, 17, 18], for entropy-constrained quantizers. We are not aware of any work which incorporates the ℓ_∞ constraint alongside.

The proposed image coder obtains good rate-distortion performance in both ℓ_2 and ℓ_∞ metrics and also it increases the rate granularity. Compared with JPEG 2000, the new method not only guarantees lower ℓ_∞ error for all bit rates, it even achieves higher PSNR for relatively high bit rates. As shown in Fig. 1d, the proposed image coder eliminates the artifacts in the image of near-lossless CALIC (1c) and at the same time it preserves the tiny feature that is removed by JPEG 2000 (Fig. 1b).

2. SCHEMATIC DESCRIPTION OF THE PROPOSED CODER

Since the proposed coder builds upon ℓ_∞-constrained CALIC, we first briefly present the latter coding technique. As shown in the flow diagram in Fig. 2, l_∞-constrained CALIC in [5] consists of five main components: gradient-adjusted prediction (GAP), uniform quantization, context formation and quantization, context modeling, and entropy coding. Let I be the current pixel value to be encoded. The GAP module makes a prediction $\bar{I}$ of I based on the knowledge of the reconstructed pixels in a precisely defined neighbourhood. The prediction $\bar{I}$ is further improved to $\hat{I}$ by adding the conditional sample mean of the quantized prediction errors $\mu(\hat{e}|\acute{c})$ conditioned on the error modeling context $\acute{c}$. The resulting residue

Fig. 4. Example of test image: Fruits (600 × 400 pixels).

$e = I - \hat{I}$ is then quantized with a uniform scalar quantizer generating $\hat{e}$. The reconstructed pixel value $\tilde{I} = \hat{I} + \hat{e}$ and the quantized prediction residue $\hat{e}$ are fed back into the system to be used in the encoding of future pixels in the image. Finally, the sequence of quantized prediction residues is losslessly entropy coded by means of a context-based arithmetic coder. Only eight coding contexts c are used for this purpose, which are formed by quantizing an error energy estimator Δ into eight bins.

The proposed image coder, shown in Fig. 3, replaces the uniform quantizer of prediction errors in near-lossless CALIC by scalar quantizers optimized for each individual coding context. The optimization problem aims at minimizing a weighted sum of the average ℓ_2 distortion and average entropy over all eight coding contexts, while preserving a maximum error bound for each prediction error.

3. OPTIMAL CONTEXT-BASED QUANTIZATION OF PREDICTION ERRORS

In order to formulate the problem we first need to introduce some notations. The set to be quantized is $\mathcal{E} = \{e_n\}_{n=1}^{N}$, where $e_n = -2^B + n$, $N = 2^{B+1} - 1$ and B is the number of bits used per pixel in the raw image. Let the quantizer partition be $\mathcal{P} = \{\mathcal{C}_1, \mathcal{C}_2, \ldots, \mathcal{C}_K\}$, for some $K \geq 1$, where $\mathcal{C}_i = (a_{i-1}, a_i] = \{e_n \mid a_{i-1} < n \leq a_i\}$ for $0 = a_0 < a_1 < \cdots < a_K = N$. Further, let y_i denote the reproduction value corresponding to codecell $\mathcal{C}_i$. Keeping in mind the optimization criterion of minimizing a weighted sum of the ℓ_2 distortion and entropy, while obeying an ℓ_∞ bound of τ, we determine y_i as follows

$$y_i = \underset{y \in \mathcal{E}, |e_n - y| \leq \tau, e_n \in \mathcal{C}_i}{\arg\min} \sum_{e_n \in \mathcal{C}_i} p(e_n)(e_n - y)^2, \qquad (1)$$

where $p(e_n)$ is the probability of the prediction residue e_n.

First of all, for the solution to (1) to exist, we must have $(a_i - a_{i-1}) \leq (2\tau + 1)$ for all i. Then the optimal solution to (1) is given by

$$y_i = \begin{cases} (e_{a_{i-1}} + 1) + \tau, & \text{if } (\mu(\mathcal{C}_i) - (e_{a_{i-1}} + 1)) > \tau \\ e_{a_i} - \tau, & \text{if } (e_{a_i} - \mu(\mathcal{C}_i)) > \tau \\ [\mu(\mathcal{C}_i)], & \text{otherwise,} \end{cases}$$

where $\mu(\mathcal{C}_i) = \sum_{e_n \in \mathcal{C}_i} p(e_n) \frac{e_n}{p(\mathcal{C}_i)}$, $p(\mathcal{C}_i) = \sum_{e_n \in \mathcal{C}_i} p(e_n)$, and $[\mu(\mathcal{C}_i)]$ denotes the closest integer to $\mu(\mathcal{C}_i)$.

By optimizing the reproduction codewords for each encoder partition via (1), the ℓ_2 distortion and the output entropy corresponding to a quantizer become only functions of the encoder partition. Let us define the ℓ_2 distortion and the entropy for each codecell $\mathcal{C}_i$ as $d(\mathcal{C}_i) = \sum_{e_n \in \mathcal{C}_i} p(e_n)(e_n - y_i)^2$ and $r(\mathcal{C}_i) = -p(\mathcal{C}_i) \log_2 p(\mathcal{C}_i)$, respectively. Then the ℓ_2 distortion and the entropy corresponding to a quantizer with encoder partition $\mathcal{P}$ are $D(\mathcal{P}) = \sum_{\mathcal{C} \in \mathcal{P}} d(\mathcal{C})$ and $R(\mathcal{P}) = \sum_{\mathcal{C} \in \mathcal{P}} r(\mathcal{C})$. Now let us denote by $\mathcal{P}_m$ the encoder partition corresponding to the scalar quantizer for coding context c_m, where $1 \leq m \leq M$, with $M = 8$ for near-lossless CALIC. Subsequently, let D_T and R_T, respectively, denote the expected ℓ_2 distortion and entropy of all quantizers over all M contexts as follows

$$D_T = \sum_{m=1}^{M} q(c_m) D(\mathcal{P}_m), R_T = \sum_{m=1}^{M} q(c_m) R(\mathcal{P}_m), \qquad (2)$$

where $q(c_m)$ is the probability of context c_m. It is important to note that in the computation of $D(\mathcal{P}_m)$ and $R(\mathcal{P}_m)$, the probability $p(e_n)$ is the conditional probability of residual e_n conditioned on context c_m.

After having established the above notations we can now formulate our task as the optimization problem

$$\min_{\{\mathcal{P}_1, \mathcal{P}_2, \ldots, \mathcal{P}_M\}} \quad D_T + \gamma R_T, \qquad (3)$$

for some $\gamma > 0$, where the optimization is performed over all possible M-tuples of partitions $\mathcal{P}_1, \mathcal{P}_2, \ldots, \mathcal{P}_M$ with codecells of maximum size $2\tau + 1$. It is easy to see that (3) can be solved by individually minimizing $J(\mathcal{P}_m, \gamma)$ for each context c_m, where $J(\mathcal{P}_m, \gamma) = D(\mathcal{P}_m) + \gamma R(\mathcal{P}_m)$. Further, notice that $J(\mathcal{P}_m, \gamma)$ is additive over codecells, in other words, the following holds

$$J(\mathcal{P}_m, \gamma) = \sum_{\mathcal{C} \in \mathcal{P}_m} (d(\mathcal{C}) + \gamma r(\mathcal{C})). \qquad (4)$$

The above additivity property allows for minimizing (4) by solving a minimum weight path problem in a weighted directed acyclic graph (WDAG) G. This graph model is similar in spirit to that used in [18], with the notable difference that in [18] the ℓ_∞ constraint was not imposed. The set of vertices of G is $V = \{0, 1, \ldots, N\}$ and the set of edges is $E = \{(x, y) | 0 \leq x < y \leq N, y - x \leq 2\tau + 1\}$. Each edge (x, y) represents a possible codecell $\mathcal{C} = (x, y]$ and the weight assigned to the edge is $w(x, y) = d(\mathcal{C}) + \gamma r(\mathcal{C})$. It is clear that any path in the graph G from 0 to N is in unique correspondence with a partition $\mathcal{P}_m$, whose cost $J(\mathcal{P}_m, \gamma)$ equals the weight of the path. Thus, minimizing (4) is equivalent to solving the minimum weight path problem in G, which can be done in $O(\tau^2 N)$ (accounting for the computation of edge weights as well). Consequently, solving (3) requires

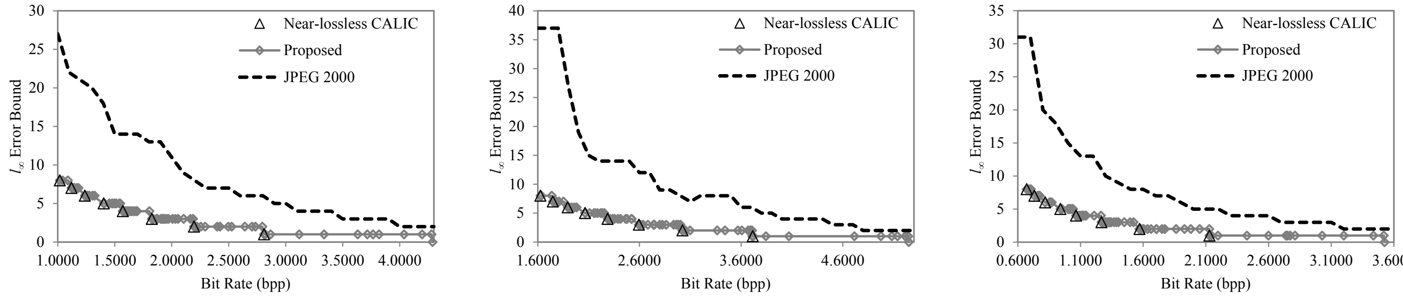

(a) Flowers (b) Plants (c) Fruits

Fig. 5. ℓ_∞ error bound of test images compressed at different rates.

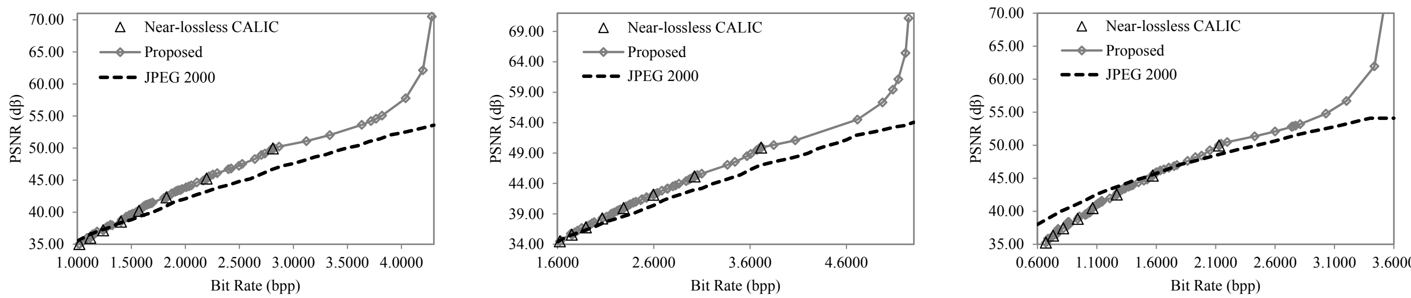

(a) Flowers (b) Plants (c) Fruits

Fig. 6. PSNR of test images compressed at different rates.

$O(\tau^2 MN) = O(N)$ since τ and M are upper bounded by a constant.

4. EXPERIMENTAL RESULTS

A training set of four 8-bit high resolution images, were used to obtain the probability distributions of prediction errors for every context c_m and every value of $\tau \in \{1, 2, \cdots, 8\}$. When collecting these data the unquantized pixel values were used in the prediction. Further, each distribution was approximated by a Laplacian distribution centered at zero. For each $\tau \in \{1, 2, \cdots, 8\}$, we have solved (3) for a decreasing sequence of values of γ, starting with some high value $\gamma_{0,\tau}$. For each τ the partitions $\mathcal{P}_1^*, \mathcal{P}_2^*, \ldots, \mathcal{P}_M^*$, corresponding to the optimal solution for $\gamma_{0,\tau}$, are very close or even identical to the uniform quantizers in near-lossless CALIC, which have the largest possible step size of $(2\tau+1)$. We will denote by $R_0(\tau)$ the value of R_T corresponding to this solution. Then all the values R_T achieved for the same τ are larger than $R_0(\tau)$. Furthermore, one has $R_0(\tau+1) < R_0(\tau)$. Further, in order to proceed to testing the proposed coder on real images we have selected for each τ only those M-tuples of partitions corresponding to entropies R_T satisfying the condition $R_0(\tau) \leq R_T < R_0(\tau - 1)$.

We have performed a comparison with near lossless CALIC and JPEG 2000, in terms of ℓ_2 and ℓ_∞ performance. One of the test images is presented in Fig. 4.

Fig. 5 plots the ℓ_∞ error bound versus bit rate, demonstrating the superiority of the proposed coder over JPEG2000 for all achievable bit rates. Fig. 6 plots the PSNR versus bit rate. As can be seen, the proposed coder achieves all possible bit rates of near-lossless CALIC with equal PSNR, plus many more intermediate bit rates; the former generates a monotonically increasing PSNR-rate function having much denser data points than the latter. Furthermore, the proposed coder outperforms JPEG2000 even in ℓ_2 metric if rates are sufficiently high.

5. REFERENCES

[1] A. Zandi, J.D. Allen, E.L. Schwartz and M. Boliek, "CREW: Compression with Reversible Embedded Wavelets," *Proc. Data Compression Conf. (DCC)*, 1995, vol., no., pp.212-221, 28-30 Mar. 1995.

[2] A. Said and W.A. Pearlman,"An image multiresolution representation for lossless and lossy compression,"

IEEE Trans. on Image Process., vol.5, no.9, pp.1303-1310, Sep. 1996.

[3] K. Chen and T.V. Ramabadran, "Near-lossless compression of medical images through entropy-coded DPCM," *IEEE Trans. on Medical Imaging*, vol.13, no.3, pp.538-548, Sep. 1994.

[4] L. Ke and M.W. Marcellin, "Near-lossless image compression: minimum-entropy, constrained-error DPCM," *IEEE Trans. on Image Process.*, vol.7, no.2, pp.225-228, Feb. 1998.

[5] *A Context-Based, Adaptive, Lossless/Nearly-Lossless Coding Scheme for Continuous-Tone Images*, ISO/IEC Standard JTC 1.29.12, 1995.

[6] X. Wu and N. Memon, "Context-based, adaptive, lossless image coding," *IEEE Trans. on Commun.*, vol.45, no.4, pp.437-444, Apr. 1997.

[7] X. Wu and P. Bao, "L_∞ constrained high-fidelity image compression via adaptive context modeling," *IEEE Trans. on Image Process.*, vol.9, no.4, pp.536-542, Apr. 2000.

[8] X. Wu, J. Zhou and H. Wang, "High-Fidelity Image Compression for High-Throughput and Energy-Efficient Cameras," *Data Compression Conf. (DCC)*, 2011, vol., no., pp.433-442, 29-31 Mar. 2011.

[9] J. Max, "Quantizing for minimum distortion," *IRE Trans. on Inform. Theory*, vol.6, no.1, pp.7-12, Mar. 1960.

[10] S. Lloyd, "Least squares quantization in PCM," *IEEE Trans. on Inform. Theory*, vol.28, no.2, pp. 129- 137, Mar. 1982.

[11] J. D. Bruce, "Optimum quantization," Sc. D. thesis, M. I. T., May 14, 1964.

[12] D. K. Sharma, "Design of absolutely optimal quantizers for a wide class of distortion measures," *IEEE Trans. on Inform. Theory*, vol. IT-24, pp. 693-702, Nov. 1978.

[13] X. Wu, "Optimal Quantization by Matrix Searching," *J. of Algorithms*, 12(1991), vol.12, no. 4, pp. 663-673, Dec. 1991.

[14] S. Dumitrescu and X. Wu, "Algorithms for optimal multi-resolution quantization," *J. of Algorithms*, 50(2004), vol. 50, no. 1, pp. 1-22, Jan. 2004.

[15] S. Dumitrescu and X. Wu, "Lagrangian Optimization of Two-description Scalar Quantizers," *IEEE Trans. on Inform. Theory*, vol. 53, no. 11, pp. 3990-4012, Nov. 2007.

[16] P.A. Chou, T. Lookabaugh and R.M. Gray, "Entropy-constrained vector quantization," *IEEE Trans. on Acoustics, Speech and Signal Processing*, vol.37, no.1, pp.31-42, Jan. 1989.

[17] H. Khalil, K. Rose and S. L. Regunathan, "The Asymptotic Closed-Loop Approach to Predictive Vector Quantizer Design with Application in Video Coding," *IEEE Trans. on Image Process.*, vol. 10, no. 1, pp. 15-23, Jan. 2001.

[18] D. Muresan and M. Effros, "Quantization as Histogram Segmentation: Optimal Scalar Quantizer Design in Network Systems," *IEEE Trans. on Inform. Theory*, vol.54, no.1, pp.344-366, Jan. 2008.